High-Performance Hydrogen-Fueled Internal Combustion Engines: Feasibility Study and Optimization via 1D-CFD Modeling

energies

MDPI

Article

High-Performance Hydrogen-Fueled Internal Combustion Engines: Feasibility Study and Optimization via 1D-CFD Modeling

Daniela A. Misul *, Alex Scopelliti and Mirko Baratta *

Energy Department, Politecnico di Torino, 10129 Torino, Italy; alex.scopelliti@polito.it
* Correspondence: daniela.misul@polito.it (D.A.M.); mirko.baratta@polito.it (M.B.)

Abstract: Hydrogen-powered mobility is believed to be crucial in the future, as hydrogen constitutes a promising solution to make up for the non-programmable character of the renewable energy sources. In this context, the hydrogen-fueled internal combustion engine represents one of the suitable technical solutions for the future of sustainable mobility. As a matter of fact, hydrogen engines suffer from limitations in volumetric efficiency due to the very low density of the fuel. Consequently, hydrogen-fueled ICEs can reach sufficient torque and power density only if suitable supercharging solutions are developed. Moreover, gaseous-engine performance can be improved to a great extent if direct injection is applied. In this perspective, a remarkable know-how has been developed in the last two decades on NG engines, which can be successfully exploited in this context. The objective of this paper is twofold. In the first part, a feasibility study has been carried out with reference to a typical 2000cc SI engine by means of 1D simulations. This study was aimed at characterizing the performance on the full load curve with respect to a baseline PFI engine fueled by NG. In this phase, the turbocharging/supercharging device has not been included in the model in order to quantify the attainable benefits in the absence of any limitation coming from the turbocharger. In the second part of this paper, the conversion of a prototype 1400cc direct injection NG engine, running with stoichiometric mixture, to run on a lean hydrogen combustion mode has been investigated via 1D simulations. The matching between engine and turbocharger has been included in the model, and the effects of two different turbomatching choices have been presented and discussed.

Keywords: hydrogen; decarbonization; sustainable mobility; direct injection; turbocharging

Citation: Misul, D.A.; Scopelliti, A.; Baratta, M. High-Performance Hydrogen-Fueled Internal Combustion Engines: Feasibility Study and Optimization via 1D-CFD Modeling. *Energies* **2024**, *17*, 1593. https://doi.org/10.3390/en17071593

Academic Editor: Anastassios M. Stamatelos

Received: 2 March 2024
Revised: 21 March 2024
Accepted: 24 March 2024
Published: 26 March 2024

1. Introduction and Background

The global clean energy transition is accelerating, driven by a combination of policy, technological change and economics. The need to reduce greenhouse gas emissions drastically and urgently has become apparent to most public institutions, governments and public opinion [1]. Moreover, the recent global energy crisis has evidenced a few concerns about energy security, with specific reference to the supply of conventional fuels such as oil and gas [2]. This has further strengthened the need and policy support for clean energy technologies [3]. The latter can benefit from the established use of hydrogen as an energy carrier, which is a valuable option for increasing the exploitation of renewable energy sources (RES). The use of hydrogen, being a carbon-free fuel, is in fact being considered as one of the pathways to promote the transition towards a sustainable energy system [4,5]. With specific reference to the transportation sector, electric cars will have higher total cost of ownership (TCO) [6] and offer shorter driving ranges than IC-powered ones in most cases. Hydrogen-fueled (H_2-fueled) internal combustion engines are considered as one of the most interesting alternatives to the BEV technology to achieve the ambitious target of the decarbonization of the transport sector [7]. As a matter of fact, IC engines are expected to retain a significant market share until 2040 [8], although the recent decision from the EU

to ban any new car with a non-zero carbon footprint is expected to have an impact on the light vehicles market in the mid- or long-term perspective. Hydrogen has a higher energy storage potential with respect to batteries, in spite of serious concerns arising regarding onboard storage. As an energy carrier, hydrogen can be exploited in fuel-cell (FC) or IC engine-powered vehicles. With respect to FCs, H_2-ICE vehicles feature an efficiency gap, which is, however, continuously being reduced. At the same time, H_2-ICEs benefit from a few remarkable advantages. First, they have significantly lower operating costs than FCs and feature a very high reliability and technological know-how, which come from a more than one-century-long tradition [9]. Second, the purity requirements are less stringent than in fuel cells, allowing for the exploitation of hydrogen coming as a side-product in many production processes [4]. Finally, hydrogen engines can benefit from the state of the art on dedicated, monofuel, NG engines [10,11], which have been developed to a great extent since the 1990s. An exhaustive review of advantages and drawbacks of the H_2-ICE, as well as a thorough overview of the measures for the engine design or conversion, is provided in [4] and, more recently, in [12–14]. Several studies have been published, focused on experimental studies, conversion of existing engines to run on H_2 as well as numerical investigation and feasibility analyses [15–23].

Jilakara et al. [15] performed a preliminary investigation by means of 1D modeling and used the obtained indications in order to successfully convert a CNG engine to run on hydrogen. Sopena et al. [16] converted a commercial gasoline 1.4 L engine to run on hydrogen, paying particular attention to the NOx emissions and the engine thermal efficiency optimization. Combustion timing and relative A/F ratio were optimized with this purpose; however, in the absence of a suitable supercharging strategy, the rated torque was limited by the low fuel density. The key role of the supercharging and the need of properly designing the turbocharger was also pointed out by Bao et al. [17], who made experimental work on a 2.0 L direct injection engine, which was derived by modifying an original, naturally aspirated gasoline engine. In this framework, a remarkable know-how has been developed in the last two decades on NG engines, with specific reference to the turbomatching-related aspects [18–20], as well as on combustion characterization and its dependence on hydrogen doping [21–23]. It is worth mentioning that blending natural gas with hydrogen can be one effective compromise between the opportunity of promoting hydrogen penetration and the current infrastructure limitations. Hydrogen-blended methane leads to significant benefit, as the experimental evidence reported in [21], together with the outputs of the heat release analysis, assessed for increased performance and stability for the engine running on an 85% NG, 15% H_2 blend. The hydrogen addition was found to lead to reduced burn duration and cycle-to-cycle variation, as well as to increased engine efficiency and higher EGR tolerance [22]. The latter can allow successful diluted, stoichiometric operation and engine de-throttling at partial load [23].

A remarkable research effort has been concentrated on natural-gas direct injection [11,19,24,25], which represents a promising solution to reduce the hydrogen engine performance gap with respect to gasoline. Several authors [26–31] also point out that possible issues about NOx emissions might arise in the design and calibration of hydrogen engines. In [28], a single-cylinder research engine was supercharged, substantially increasing the power output. However, to avoid backfire and pre-ignition, the air-to-fuel ratio was limited to a minimum lambda of 1.3, which would lead to unacceptable NOx emissions. Recycling part of the exhaust gases (EGR) allowed stoichiometric supercharged operation, increasing the maximum power output to gasoline levels and higher, while still enabling efficiency after treatment. Rezaei et al. [29] found that a good match of the turbocharger group is essential, since a drop in lambda value (air–fuel ratio), e.g., in the full load range or at rated power, results in a rapid increase in NOx emissions. Similarly, Bulgarini et al. [30] hinted at possible issues during transient when trade-off between power density and NOx are considered. In [31], driving cycles simulations were performed with specific focus on the trade-off between efficiency and NOx emissions. With a 3.0 L hydrogen engine, nitrogen

oxide emissions were even sufficiently low to meet the Super-Ultra-Low-Emissions Vehicle II emissions specification.

The development of hydrogen-fueled engines still requires further research on each of the aspects discussed above, as well as on the trade-off optimizations amongst them. At the same time, it holds a great potential both in the transition phase (through the introduction of NG/H_2 blends) and as a feasibility solution for a carbon-free mobility.

2. Present Work

The present paper aims at providing a model-based quantitative feasibility study on the achievable performance from a hydrogen engine, providing some insight into the required turbocharger performance and the most relevant control variables. A lot of effort has been devoted recently to the development of this technology; however, there are a lot of parameters to be optimized and many design concepts to be considered (among others, direct- or port-injection, lean or EGR-diluted combustion, combustion chamber design). The results obtained in the literature might thus be affected by the specific case study and by the choices, which have been made in terms of relevant variables and constraints of the optimization processes. For the above reasons, the aim of this paper is to propose a systematic study in order to understand the potential for an H_2-powered engine to be competitive with its conventional engine counterparts, as well as with fuel-cell or battery electric vehicles. On one hand, this study has been limited to the combustion and performance-related variables in order to better fix the targets of the analysis. On the other hand, the effect of the main engine calibration variables has been investigated with reference to two typical engines for passenger car application in the presence of reasonable limits for the peak firing pressure and temperature at turbine inlet.

In the first part, a typical 2000cc SI engine model was considered, and the maximum achievable engine torque was quantified, relative to a baseline, PFI, stoichiometric NG engine. The turbocharger was not included in the model in order to highlight the ideal requirements to the turbocharger device and avoid any limitation coming from it. In the second part, the conversion of a prototype high-performance engine, for which experimental data with NG fueling were available [10,25], was investigated by quantifying the effect of different turbomatching choices on the achievable performance and efficiency.

3. Methodology and Case Studies

3.1. Numerical Approach

The engine models were built according to a 1D approach in the GT-POWER 2022 environment [32,33]. The tool is based on the discretization and solution of generalized Euler equations [33], in which heat transfer and friction effects are considered through properly defined source terms. The solution is considered zero-dimensional in specific engine parts such as cylinders, valves, injectors and turbochargers [33]. Each engine component was then modeled in order to measure its geometrical, flow and heat transfer characteristics. This includes pipes, air-box, injectors, valves and cylinders. In addition, engine 2 includes the turbocharger modeling. In particular, the heat transfer in pipes is calculated using a heat transfer coefficient, which is calculated at every timestep by using the Colburn analogy [33]. The in-cylinder heat transfer was modeled with the "WoschniGT" model included in GT-POWER: the in-cylinder heat transfer is calculated by a formula which emulates the original Woschni correlation without swirl [34]. A difference lies in the treatment of heat transfer coefficients during the period when the valves are open, where the heat transfer is increased by inflow velocities through the intake valves and also by backflow through the exhaust valves [32].

Combustion was modeled by using a non-predictive combustion model, which imposes the combustion burn rate for spark-ignition engines using a Wiebe function. The main calibration parameters are anchor angle, combustion duration and Wiebe exponent. The former is the number of crank angle degrees between TDC and the 50% combustion point of the Wiebe curve (MFB50). Duration refers to the burn duration, from 10% fuel mass

burned up to 90%. The Wiebe exponent influences the shape of the Wiebe function [32]. In GT-POWER, turbine and compressor performance are modeled using performance maps. In this case, turbochargers were included only for Engine 2, and maps were the ones of the real turbocharger. Both compressor and turbine maps are a series of performance data points, each of which describes the working condition by speed, pressure ratio, mass flow rate and thermodynamic efficiency [33].

3.2. Part 1: 2000cc 4-Cylinder Engine Model

The first part of the activity was focused on a 4-cylinder SI engine, whose map in the GT-Power environment is shown in Figure 1. The engine features an overall displacement of 2000cc, and two different CR have been considered for the analysis. An overview of the engine characteristics is given in Table 1.

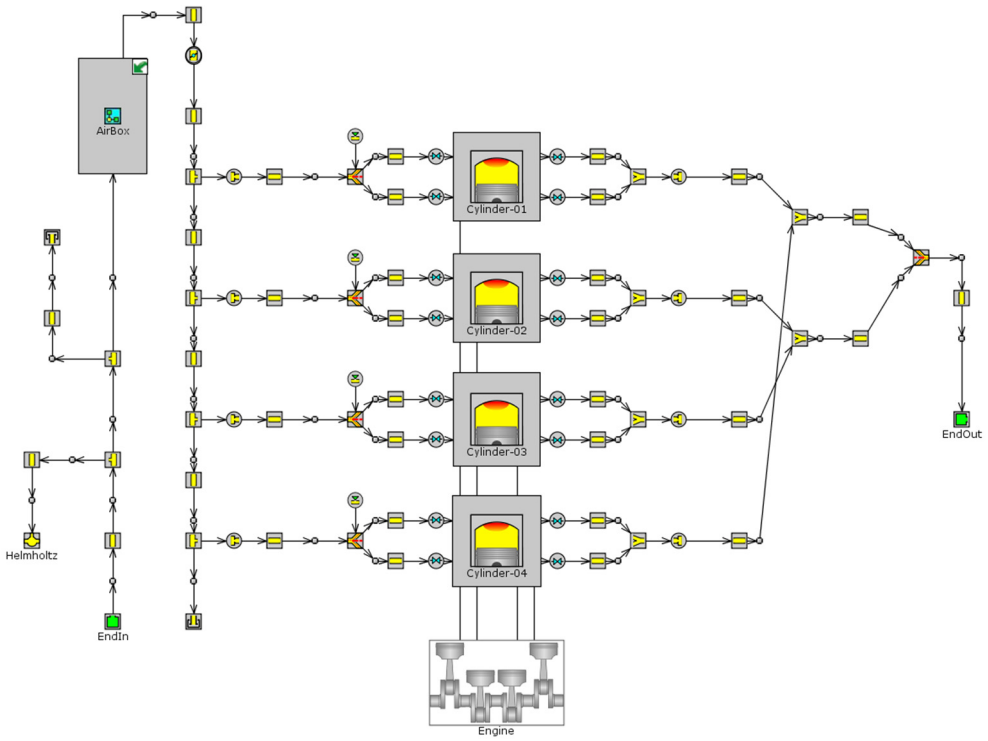

Figure 1. Map of the reference engine #1 in GT-Power.

Table 1. Engine 1 characteristics.

Displaced volume	2000cc
Compression ratio	9.5–11.5
Number of valves per cylinder	4
Valve lift	Fixed
Fuel injection	PFI (NG) DI (H_2)
Lambda	1 (NG) 2 (H_2)
Turbocharger modeling strategy	'Imposed boost' with $p_{trb,in} \approx p_{boost}$

The engine modeling approach was purposely selected so as to maximize the model flexibility. In particular:

- The Wiebe function was used to model the combustion. The MFB50 position was identified as the most relevant combustion parameter, affecting peak firing pressure, torque and bsfc. The MFB50 was hence used as a parameter in the considered investigation, whereas the Wiebe exponent and the combustion duration were maintained at 2 and 30 deg CA, respectively.

- The turbocharger was not included in the model, but the pressure at the model input was imposed so as to reproduce the effect of a compressor. At the same time, the backpressure imposed by the turbine was taken to be the same as the imposed boost pressure. This choice was motivated by the opportunity to maximize the model flexibility by highlighting the ideal requirements to the turbocharger device rather than suffering from any limitation coming from it.

3.3. Part 2: Full Turbocharged Engine with VVA and Direct Gas Injection

The second part of the investigation, which was kept within a 1D simulation framework, was devoted to the feasibility study of the conversion of an existing prototype engine to run on hydrogen. The engine design is the result of the cooperation of the authors' research group with Fiat Research Center, BorgWarner, AVL List GmbH within the GasOn research project [10,25] and features a direct injection concept, variable valve actuation and high structural integrity, which allowed a high CR to be adopted. A list of the main engine characteristics is reported in Table 2.

Table 2. Engine 2 characteristics.

Displaced volume	1368cc
Compression ratio	13
Number of valves per cylinder	4
Valve lift	Hydraulic VVA system (MultiAir)
Fuel injection	DI
Lambda	1 (NG) 1-2 (H_2)
Turbocharger modeling strategy	Full turbocharger model included

The 1D model of the engine was calibrated against experimental results in the NG functioning, with reference to a few steady-state working points. In particular, the Wiebe function parameters were calibrated in each operating point by seeking the best compromise between the pressure curves of the different cylinders. The combustion model parameters were kept constant in each operating point to perform the simulations with hydrogen. This assumption was justified by the fact that the different burning characteristics can be compensated to some extent by a suitable variation in the spark timing management, which allows the possibility to keep the MFB50 timing unchanged. Moreover, it was verified that the combustion duration and the Wiebe exponent retained a minor influence on the main combustion-related variables with respect to the MFB50 angular position.

4. Engine 1 Results and Discussion

4.1. Baseline CNG Engine Definition

As a first step, a baseline configuration was defined with reference to NG fueling in order to allow a fair assessment of the engine performance,. A PFI injection system and a stoichiometric A/F ratio were selected. The achievable performance was thus quantified with reference to a few structural limitations. More specifically, the peak firing pressure (PFP) and the exhaust temperature were limited to 90 bar and 950 °C, respectively.

As far as the baseline NG engine full-load curve, actually, two possible choices can be made, namely a bmep-optimized and a bsfc-optimized one. In the first case, it was observed that the maximum bmep output was obtained by increasing the boost level while retarding the MFB50 angle in order to keep the PFP under the 90 bar limit. In the second case, the optimal bsfc required a combustion phasing much closer to the MBT timing (around 10 deg CA after TDC).

Figure 2 shows the dependence of bsfc on MFB50 timing and boost level for the working condition at 3000 rpm, full load. For a given MFB50, a higher boost determines a better overall efficiency, as the friction losses retain a reduced importance. As the boost is reduced, the limit in MFB50 for which the maximum PFP is approached decreases (red circles in Figure 2). This allows a better combustion phasing to be actuated and finally leads

to a decrease in the fuel consumption. It can also be deduced that with boost = 2 bar, the optimal combustion timing has been almost reached, thus suggesting that further benefit can hardly be obtained from boost levels lower than 2 bar. The latter value was then taken as the lower bound when the bsfc-oriented calibration was defined.

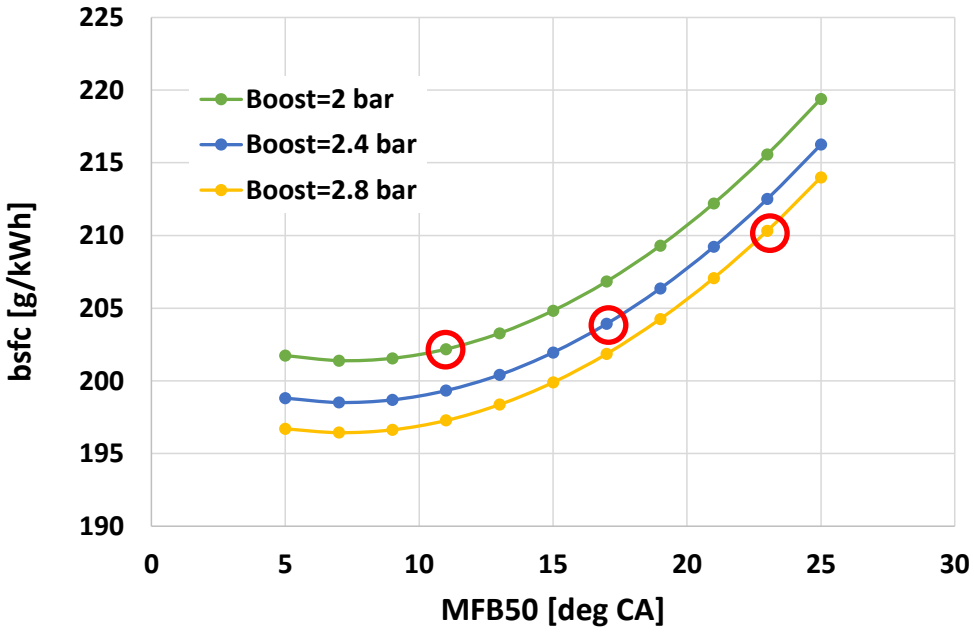

Figure 2. Engine 1: bsfc as a function of MFB50 for different boost levels at 3000 rpm, full load. Red circles indicate the combination in which the limit of PFP is approached.

The results of the two different optimization strategies are presented hereafter, in Figures 3 and 4. Figure 3 shows a comparison of the in-cylinder pressure traces, which were obtained for the 'bmep-oriented' and the 'bsfc-oriented' calibrations for the engine speed of 3000 rpm and full load. Figure 4 reports the bmep and bsfc curves versus engine speed for both the considered strategies.

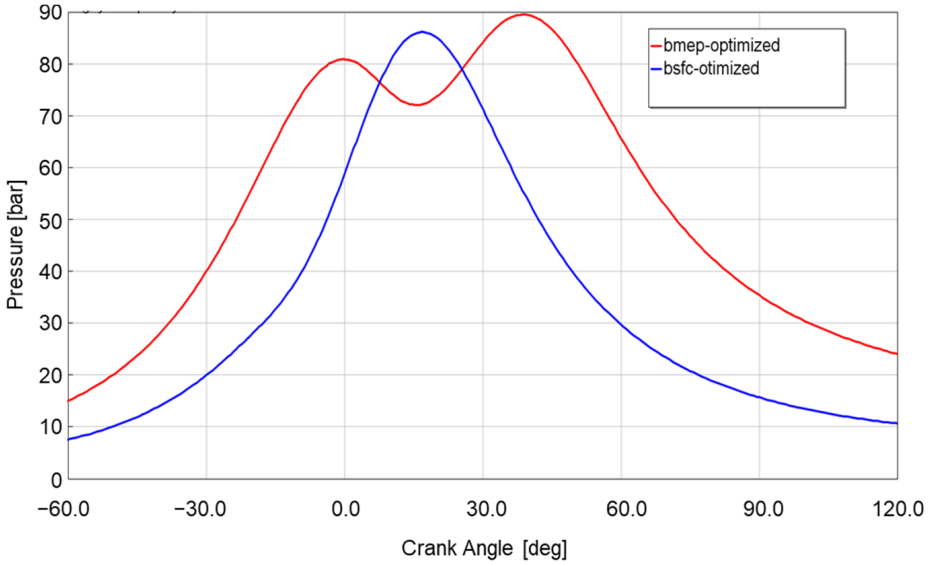

Figure 3. Engine 1: in-cylinder pressure curves at 3000 rpm, full load, for the 'bmep-optimized' and 'bsfc-optimized' strategies.

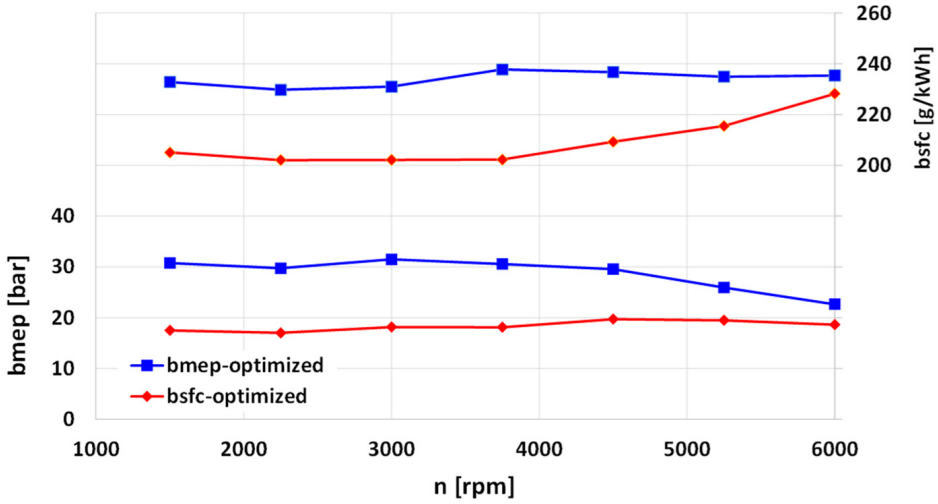

Figure 4. Engine 1: full-load curves for 'bmep-optimized' and 'bsfc-optimized' calibration.

In particular, should an 'ideal' supercharging system be available, a bmep of 30 bar can be reached for a wide range of engine speeds, despite the rather conservative PFP limit. This represents a performance enhancement from 35% to 75% with respect to the optimized bsfc strategy and is accompanied by a bsfc penalty ranging between 10% and 18%, which can be considered as acceptable for full-load operation.

The trade-off between bmep and bsfc can be significantly modified if a different choice for the engine CR is made. An example is given in Figure 5, where the results from the bmep-optimized calibration are compared for the volumetric compression ratio of 9.5 and 11.5. In this case, the engine with increased CR benefits from the improved theoretical A/F cycle efficiency, but it also suffers from a less favorable combustion timing. The engine with CR = 11.5 can approach nearly the same bmep output as the reference value CR = 9.5 while keeping a modest bsfc increase with respect to the 'bsfc-optimized' strategy with baseline CR (Figure 4). The bmep curve obtained from the 'bmep-optimized' calibration, with CR = 9.5, was finally considered for defining the baseline full-load curve to be used as reference for the H_2 engine performance assessment. This choice has been motivated by the opportunity to show the potential of a somehow 'base' engine from a technological point of view. The effect of an increased CR can be beneficial; however, this will need to be further analyzed in Section 4.

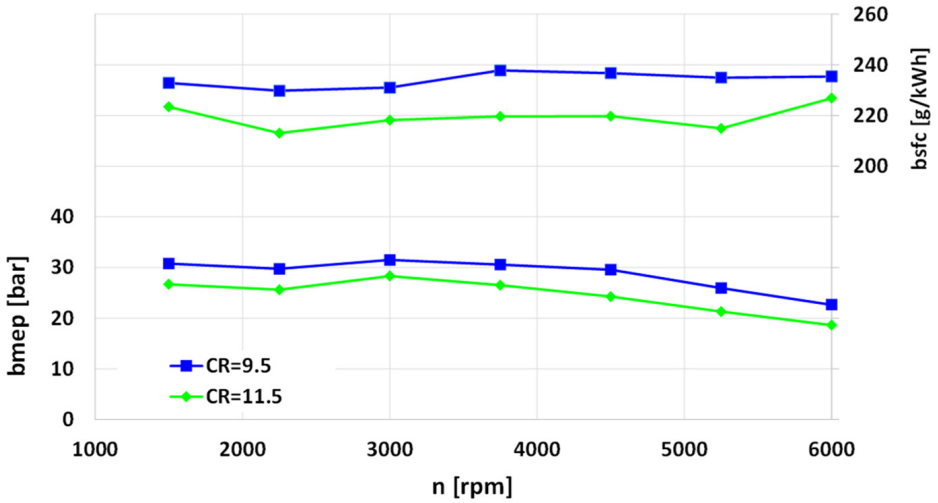

Figure 5. Engine 1: full-load curves for 'bmep-optimized' calibration, CR = 9.5 vs. CR = 11.5.

4.2. Full-Load Curve under H_2 Fueling

In this section, the full-load performance of the engine fueled with hydrogen will be compared to the baseline NG configuration, as defined in the previous section. Table 3 summarizes the main changes made when hydrogen was implemented in the model.

Table 3. Engine 1 model settings.

	NG Engine	**H_2 Engine**
Lambda	1	2
Fuel injection strategy	PFI	DI
EOI timing [deg CA]	−180	−70
MFB50 timing, boost pressure	Adjusted so as to maximize performance and comply with the p and T limits	

First of all, as hydrogen is well suited for lean operation, it was decided to fix the relative A/F ratio, λ, to the value of 2 based on the indications from the literature [4]. This choice is reported to be beneficial for fuel consumption and allows the NOx emissions and the engine thermal stress to be reduced to a great extent [28,29]. Second, the DI injection strategy was considered for the H_2 engine in order reduce the effect of the lower fuel density with respect to methane [24,25]. The EOI timing was set at −70 deg CA, which allows the volumetric efficiency to be maximized at low-end torque operating conditions, still keeping a reasonable time available for fuel–air mixing [10,25].

Figure 6 provides an example of comparison between the indicated cycles relative to the H_2 and the NG fueling for the same operating condition (3000 rpm and full load). Both cycles were obtained by maximizing the bmep output in the considered case. It is apparent that the in-cylinder pressure curve is steeper than that of NG during the compression stroke (Figure 6a). This is due to the increased ratio of specific heats as well as the higher elastic gas constant of the hydrogen–air unburned mixture with respect to the baseline case. In particular, the estimated increase in the gas constant ranges around 32–33%. In the presence of a fixed PFP limit, the boost level had to be reduced by around 15% for the H_2 fueling, leading to a decrease in the in-cylinder pressure during the intake phase (Figure 6b). This is one of the reasons behind the detriment in the bmep output with respect to the baseline NG operation. It is also worth mentioning that the PFP limit has been reached by the first peak, which is essentially due to the compression effect only.

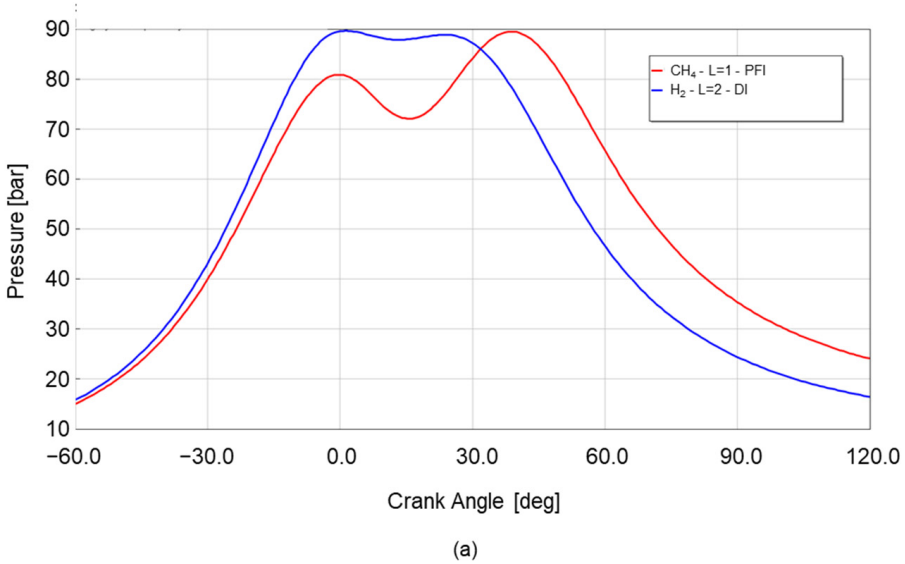

Figure 6. *Cont.*

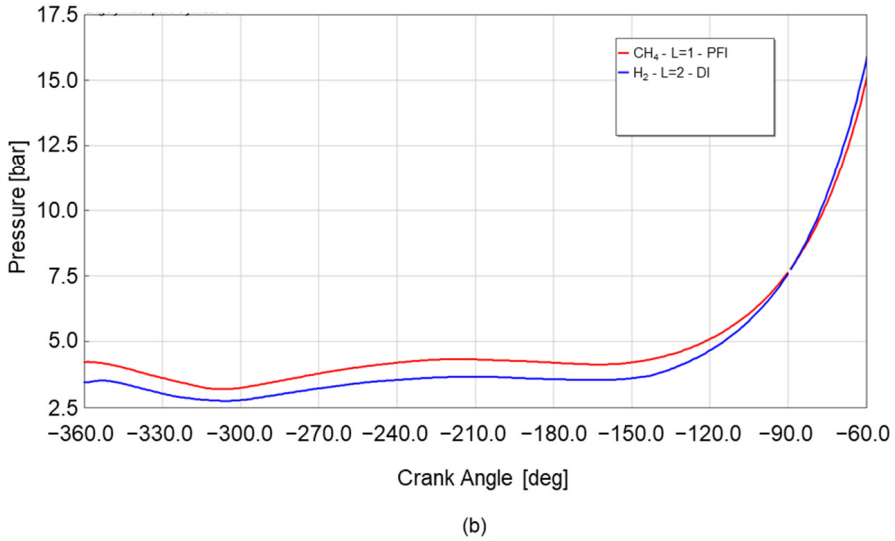

Figure 6. Comparison of the in-cylinder pressure traces at 3000 rpm, full load, for CH_4 and H_2 fueling (Cylinder #1). (**a**) Detail from −60 °CA to 120 °CA; (**b**) Detail from −360 °CA to −60 °CA.

Figure 7, which reports the value of the optimization parameters for both cases, shows that the above-mentioned behavior was observed for engine speed ranging from 1500 to 4500 rpm. A positive fallout of the reduced boost consists in the possibility to advance the combustion timing by around 7–10 degrees, which determines an increase in the engine-indicated efficiency. Figure 8 reports the comparison of the engine bmep and bsec (brake specific energy consumption in [MJ/kWh]). The latter was considered to be more significant than the bsfc due to the difference in LHV between the fuels. The hydrogen-powered engine showed a bmep reduction by around 35% over the entire full-load curve, which is due to both the reduction in the boost level and the decision to run lean. In addition, the absence of any turbocharger limitation led to a rather optimistic bmep curve for the NG engine. However, the absolute value of the H_2 engine bmep, 20 bar, represents a very good result. The better combustion phasing contributes to an improvement of the specific energy consumption by around 10–15%.

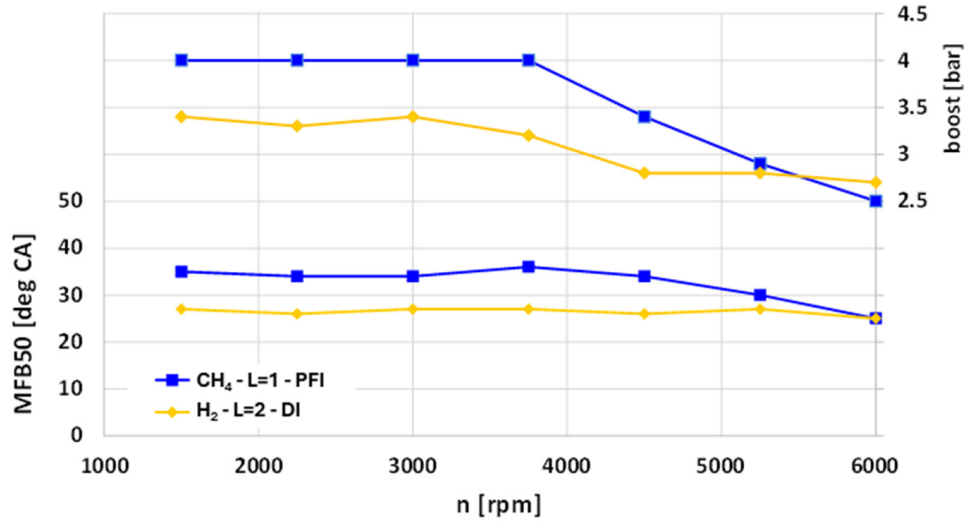

Figure 7. Model parameter optimization.

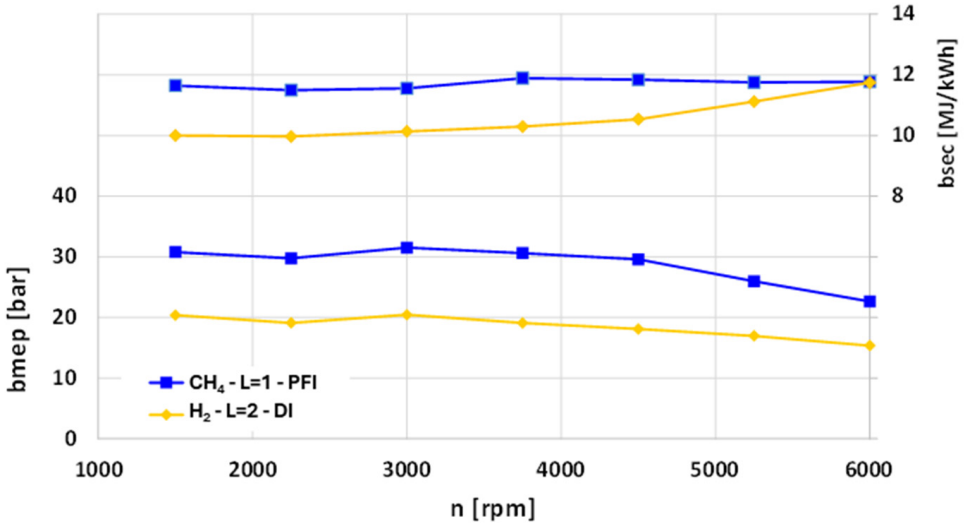

Figure 8. bmep output and bsec at full load for stoichiometric NG and lean H_2 operation.

5. Engine 2 Results and Discussion

5.1. Engine Model Calibration under CNG Fueling

In this section, the GT-Power model of the high-performance prototype 1400cc engine was calibrated against the available experimental data under NG fueling. The engine map is shown in Figure 9. Six engine working points were considered for the model calibration and analysis, as it is detailed in Table 4.

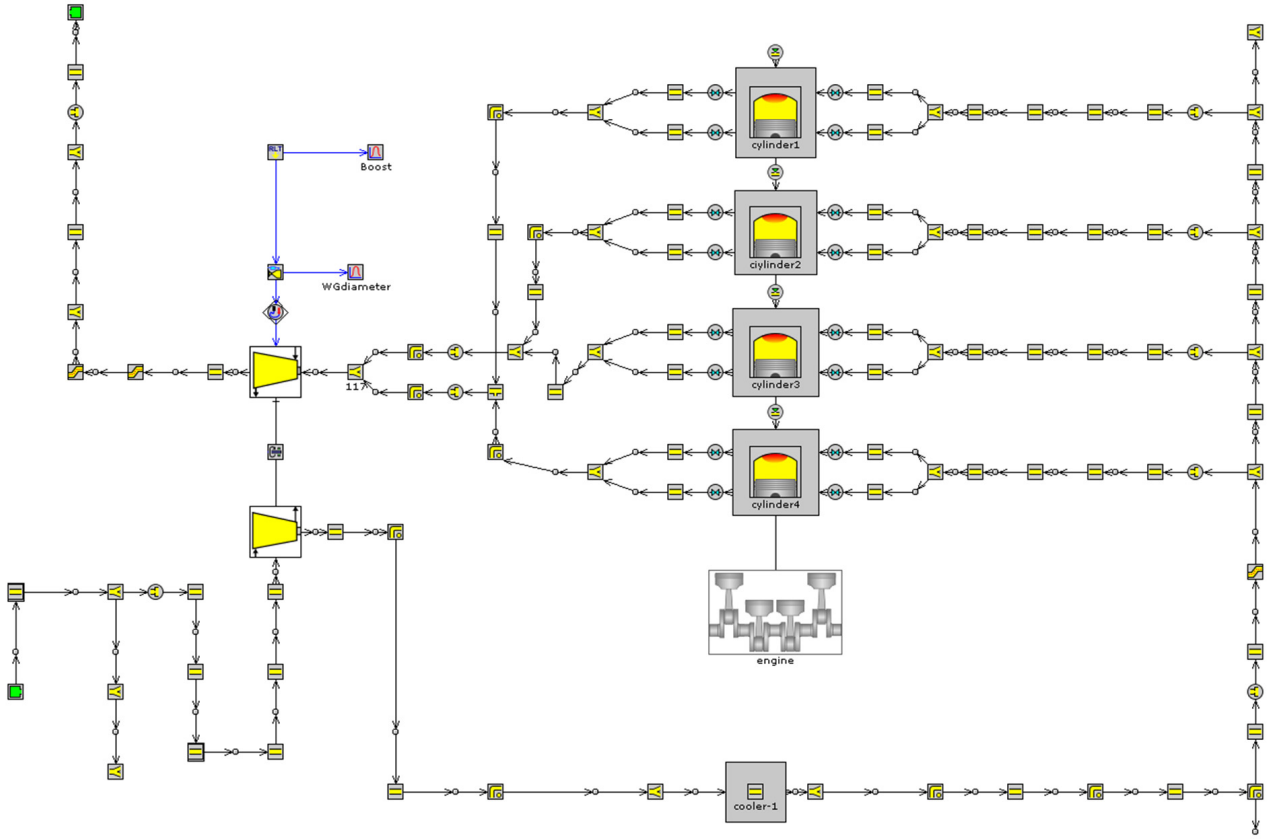

Figure 9. Map of the reference engine #2 in GT-Power.

Table 4. Engine 2 experimental working points for calibration and analysis.

Working Point #	Speed [rpm]	Load [bar]	EOI [°CA]	Exp MFB50 [°CA]
(1)	2000	4	331	7.4
(2)	2000	8	326	7.5
(3)	2500	13	102	7.9
(4)	3000	3	221	7.3
(5)	4000	5	101	7.6
(6)	2000	17 (Full load)	122	11.3

The model calibration process was mainly focused on the in-cylinder pressure and the performance related variables, given that the model was oriented to the assessment of their dependence on the fuel properties and on the combustion strategy. It was also decided to keep the combustion model as simple as possible; thus, the Wiebe function was applied. It is worth pointing out that the model formulation would need to be revised for a possible application to pollutant-formation modeling. However, in such a case, experimental results would be needed also under H_2 fueling. The procedure for the definition of the Wiebe constants in each operating point was as follows:

- TPA analysis [32] of the experimental in-cylinder pressure traces for each cylinder;
- extraction of the Wiebe parameters which suit the diagnosed heat-release profiles;
- evaluation of cylinder-averaged values for the parameters;
- Slight adjustment of the latter values in order to improve the fit with experimental results. In this phase, the value of the Wiebe exponent was fixed at 1.5 for all the operating points.

The adoption of a unique set of combustion parameters for each operating point is justified by the lack of experimental data available under hydrogen operation, and consequently by the opportunity to limit the assumptions to be made in this regard.

The results of the model validation are presented in Figures 10 and 11. Figure 10 reports the in-cylinder pressure traces for cylinder #2, with reference to a few representative test cases. The overall agreement of the pressure curve is fairly good, and the PFP values are reproduced with good accuracy. A certain deviation of the pressure curve with respect to the experimental one is anyhow apparent in the combustion development phase due to the choice of adopting a constant Wiebe exponent and to the opportunity to seek a compromise amongst the different cylinders. The most representative variables for all the cylinders, as well as the air mass-flow rate and the bmep of the engine, are reported in Figure 11 for the six considered working points. Overall, a satisfactory agreement is confirmed, which gives the model the required accuracy for a reliable estimation of the performance under hydrogen-powered conditions. In general, there is a PFP error which stems from the optimization process, which targeted a 'cylinder-averaged' cycle, and the dispersion amongst the cylinder was quite underestimated by the model. Finally, a higher deviation from the experiments was found for the bmep value at 4000x5, hinting a possible inaccuracy of the friction model coefficients at high speed.

5.2. Performance Estimation under Hydrogen Fueling

In this section, the full-load performance of the engine fueled with hydrogen will be compared to the baseline NG configuration, as defined in the previous section. This study was conducted by considering the behavior of the entire system, including the turbocharger, which represents a different approach with respect to Section 3. This approach was chosen with the purpose of highlighting the compatibility of an existing engine to the new combustion concepts, as well as of assessing the required design variants in order to optimize the attainable performance. The first considered operation point is the full-load one at 2000 rpm, which was calibrated against experimental results for methane operation. The second one was at 4000 rpm, full load, and was chosen in order to highlight possible mass-flow limitations induced by the turbine at higher speeds [17].

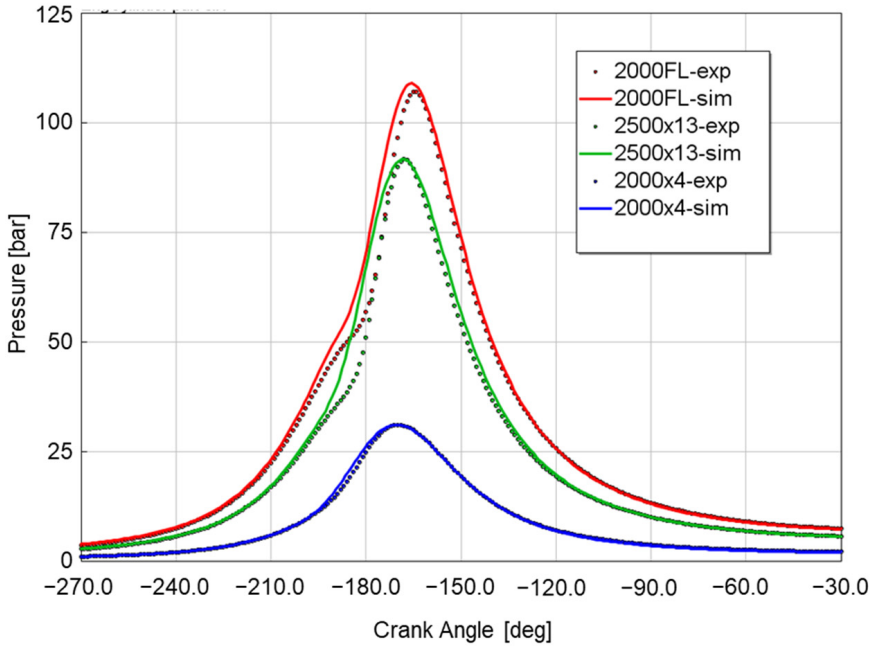

Figure 10. Model validation under NG operation: in-cylinder pressure traces for cylinder #2 in a few representative test cases. Firing TDC is at −180 deg CA.

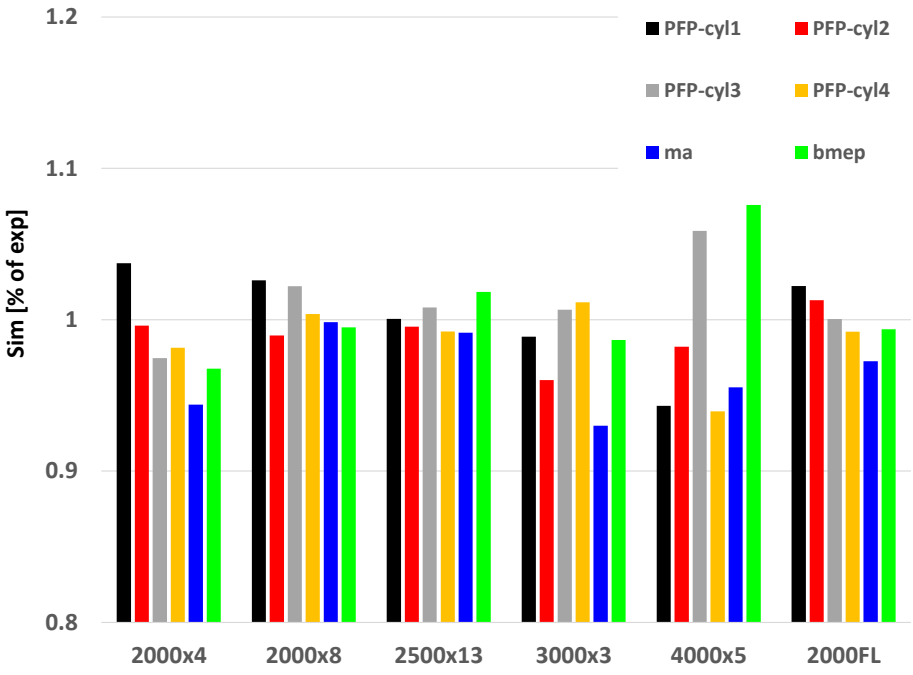

Figure 11. Model validation under NG operation: ratio of simulated to measured values for peak firing pressure, air mass-flow rate, brake mean effective pressure.

5.2.1. 2000 rpm, Full Load

Table 5 summarizes the main changes made when hydrogen was implemented in the model. The latter has been tested both with a stoichiometric and a lean mixture (for which hydrogen is well suited) in order to gain an insight into the influence of the combustion concept on the engine and turbocharger performance.

Table 5. Engine 2 model settings.

	NG Engine	H_2 Engine
Lambda	1	1–2
MFB50 timing, boost pressure, intake valves lift	Adjusted so as to maximize performance and comply with the p and T limits	

Figure 12 provides a comparison between the indicated cycles relative to the two hydrogen mixtures and the calibrated natural-gas fueling at the mentioned operating condition. As a first step, control parameters (target boost, MFB50 and nominal IVC) were left unchanged so that the effect of a simple fuel replacement could be considered. The main cycle-averaged engine performance results are reported in Table 6.

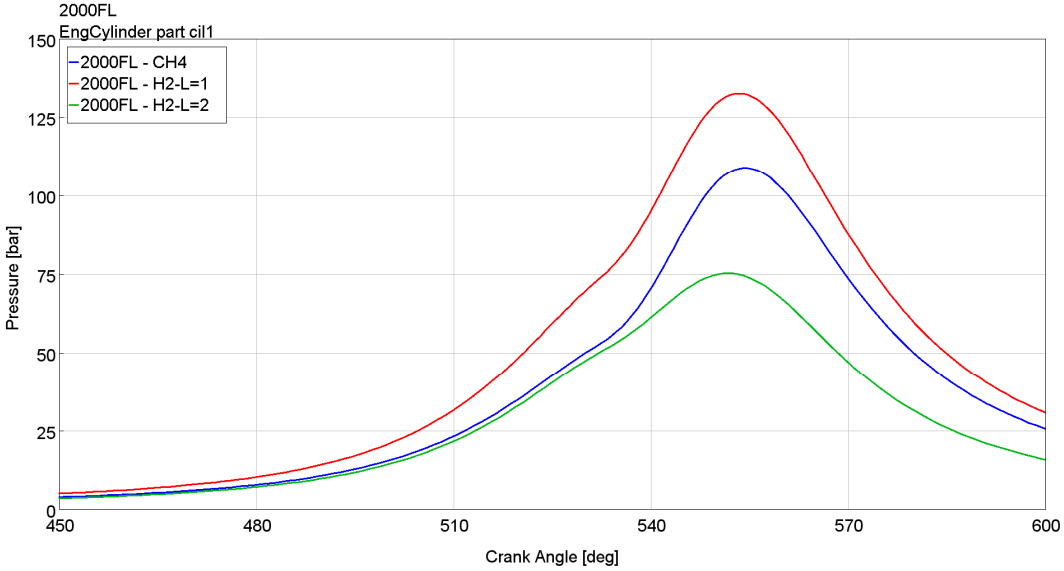

Figure 12. Comparison of the in-cylinder pressure traces at 2000 rpm, full load, for CH_4 and H_2 fueling with λ = 1 and λ = 2 (Cylinder #1). Fixed parameters: target boost = 1.7 bar, MFB50 = 10.2° CA, nominal IVC = 520 °CA.

Table 6. Results of a boost sweep for the full-load operation at 2000 rpm. Fixed parameters: target boost = 1.7 bar, MFB50 = 10.2 °CA, nominal IVC = 520 °CA.

	Average PFP	bmep	bsec	Effective Boost Pressure	Air Mass Flow Rate	Turbine Inlet Temperature	Turbine Inlet Pressure
	bar	bar	MJ/kWh	bar	g/s	K	bar
CH_4	108.9	17.4	9.7	1.7	36.7	1007	1.6
H_2 - λ= 1	132.5	20.0	10.1	1.7	36.4	1067	1.6
H_2 - λ = 2	75.3	8.2	9.9	1.4	29.3	807	1.4

The first apparent differences in the stoichiometric engine are the steeper pressure trace in the compression phase and the higher maximum in-cylinder pressure. The former is in agreement with the findings in Section 4.2 and is caused by the high ratio of specific heat of hydrogen, which increases the pressure level for a given temperature and trapped mass. During combustion, the effect is further reinforced by the higher ratio between LHV and A/Fst, with respect to NG fueling. It is worth underlining that the possible detrimental effect induced by the low fuel density is minimized by the very late injection timing (see Table 4). The hydrogen-powered engine running with λ = 2 highlighted a significant in-cylinder pressure reduction. This is due not only to the dilution effect, which

reduces the combustion temperature, but also to the reduced boost level with respect to the stoichiometric case. The decrease in the exhaust temperature at turbine inlet leads to a reduction in the available turbine power and, in turn, in the achievable boost. With specific reference to Table 6, the boost level is controlled by the wastegate in both the stoichiometric operating conditions. In the last case, the turbocharger controller reacts to the decrease in the turbine inlet temperature by fully closing the wastegate; however, this is not sufficient to avoid a significant boost level decrease. Consequently, if the same operation parameters are imposed for both combustion concepts, the bmep obtained under lean hydrogen operation reduces by around 53% compared to the stoichiometric methane engine.

The next objective of the study was devoted to reducing the torque penalty of the lean hydrogen engine with respect to the baseline, stoichiometric and NG one and possibly to restoring the original performance. Consistently with a feasibility study approach, in the absence of specific information about possible revisions of the engine structural design, it has been decided to consider the same PFP and turbine inlet temperature (TIT) limits as for the methane engine, i.e., around 110 bar and 950 °C, respectively. The goal was pursued through different steps, as described below.

1. Definition of the best trade-off between three control parameters: IVC timing, boost pressure and MFB50 angle imposed by the Wiebe function. The presence of MultiAir VVA allowed to change the lift timing of the intake valves, defined by a nominal closure value. In this regard, simulations with variable boost with given IVC showed a maximum achievable pressure at around 2 bar, pointing out a limitation coming from the turbocharger operation. Figure 13 reports a boost sweep from 1.5 bar to 2.5 bar at the indicated operating conditions. Table 7 reports the main results obtained in this analysis.

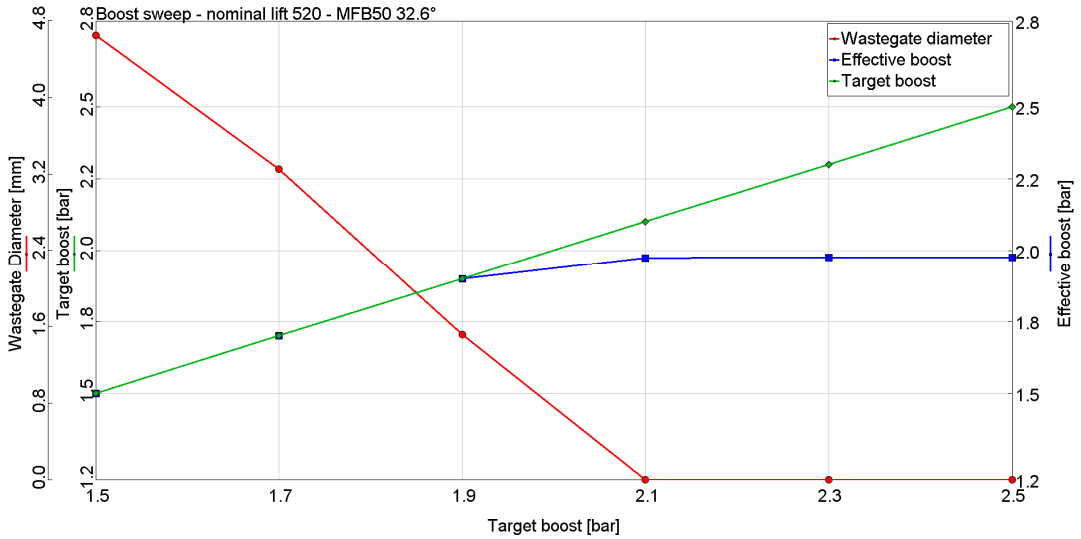

Figure 13. Effect of the change in the target boost on the effective one for hydrogen operation with λ = 2. Fixed parameters: MFB50 = 32.6 °CA, nominal IVC = 520 °CA.

Table 7. Results of a boost sweep for the full-load operation at 2000 rpm. Fixed parameters: MFB50 = 32.6 °CA, nominal IVC = 520 °CA.

MFB50 = 32.6 °CA Nominal Lift = 520 °CA						
Target Boost Pressure [bar]	**1.5**	**1.7**	**1.9**	**2.1**	**2.3**	**2.5**
Average PFP [bar]	58.1	66.4	74.7	77.7	77.8	77.8
bmep [bar]	7.7	9.0	10.3	10.8	10.8	10.8

Table 7. *Cont.*

	MFB50 = 32.6 °CA Nominal Lift = 520 °CA					
bsec [MJ/kWh]	11.3	11.1	10.9	10.9	10.9	10.9
Effective boost pressure [bar]	1.50	1.70	1.90	1.97	1.97	1.97
Air mass flow rate [g/s]	31.4	36.0	40.4	42.1	42.1	42.1
Turbine inlet temperature [K]	915	922	928	930	930	930
Turbine inlet pressure [bar]	1.46	1.61	1.77	1.83	1.83	1.83

From the results, it is clear that when trying to increase the boost beyond 1.9 bar, the wastegate completely closes, indicating a saturation condition for the controller, similarly to the behavior already observed in Figure 12 and Table 4. The result of this intermediate optimization is a bmep value of 10.8 bar.

2. The turbine size was fictitiously decreased through the introduction of a mass-flow multiplier (MFM) of 0.8 so as to increase the turbine backpressure and, in turn, the work exploitable from it. Results of a new target boost pressure sweep are shown in Figure 14 for the same engine operation parameters as Figure 13. The results testify that the target boost is successfully reached without the need of a complete closure of the wastegate valve.

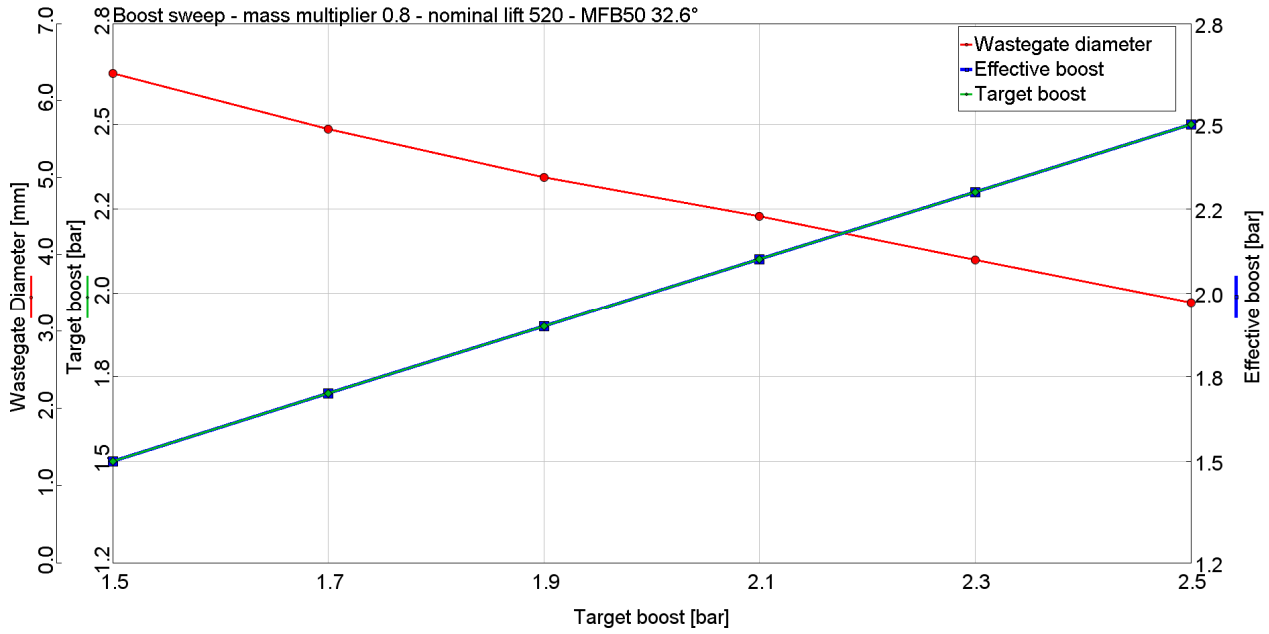

Figure 14. Effect of the change in the target boost on the effective one, for hydrogen operation with λ = 2 with turbine MFM = 0.8. Fixed parameters: MFB50 = 32.6 °CA, nominal IVC = 520 °CA.

The target boost of 2.5 bar allowed the bmep to be increased up to 13.6 bar, still remaining low compared to the original value of the methane engine.

3. Starting from the result of step 2, an optimization of the three parameters has been carried out. The boost and the MFB50 angle showed the same behavior as in Section 3, and no significant benefit could be obtained by changing the IVC timing. In fact, the actuated intake valve lift had already been optimized in the calibration phase of the methane engine as the best compromise between intake duration and backflow occurrence. Table 8 shows the results of this optimization process: it has to be noted that the boost target is not reached, but the effective boost pressure is limited to 2.66 bar.

The final bmep is 16.2 bar, with a decrease from the baseline methane engine limited to 7% and a comparable bsec value. At the same time, PFP is maintained just below the 110 bar limit, and the turbine inlet temperature is far from the limit. These results indicate that the considered engine can be successfully converted to lean hydrogen operation, as a fully decarbonized tank-to-wheel operation has been achieved, with limited penalty in the rated torque and nearly constant energy consumption.

Table 8. Results for the optimized lean H_2 engine with original (MFM = 1.0) and reduced-size turbine (MFM = 0.8).

Parameters	Average PFP	bmep	bsec	Effective Boost Pressure	Air-Mass Flow Rate	Turbine Inlet Temperature	Turbine Inlet Pressure
	bar	bar	MJ/kWh	bar	g/s	K	bar
Original turbine MFB50 = 32.6 °CA; nominal lift = 520 °CA target boost = 2.1 bar	77.7	10.8	10.9	1.97	42.1	930	1.83
Turbine MFM = 0.8 MFB50 = 32.6 °CA; nominal lift = 520 °CA target boost = 2.5 bar	99.5	13.6	10.8	2.52	53.0	951	2.48
Turbine MFM = 0.8 MFB50 = 32.6 °CA; nominal lift = 520 °CA target boost = 2.7 bar	106	16.2	9.7	2.66	56.5	902	2.67

It has to be noted that the bmep penalty is much lower than that obtained for Engine #1 in Section 3. The main reasons are as follows:

- the high CR of the engine, which limits the maximum achievable boost for both the baseline and the H_2 engine;
- the early IVC adopted at full load combined with late direct injection, which nearly eliminate any volumetric effect induced by the low hydrogen density;
- the consideration of a real engine turbocharging system, rather than an ideal one, has mitigated the effect on the bmep.

5.2.2. 4000 rpm, Full Load

In this section, a higher engine speed, 4000 rpm, is investigated. No experimental data were available at high speed, full load for methane operation. Still, considering the concerns raised in [17] and the mentioned attention to the turbomatching optimization [18–20], the purpose of this analysis was to verify any negative fallout at high speed due to the reduction of the turbine size. Both the original (MFM = 1) and the reduced-size turbine (MFM = 0.8) were considered.

A preliminary sweep of target boost pressure has been conducted with MFB50 = 7.1 °CA, nominal IVC = 420 °CA, for the original turbine configuration. The results are reported in Figure 15.

In this case, a limitation of bmep is apparent, which is due to a corresponding limit in effective boost. The limitation seems to be caused by the occurrence of the turbine speed limit, which hinders possible performance improvements. At the same time, it is also clear that the boost level should be reduced in order to meet the constraint on the PFP value. Subsequently, an optimization of the nominal lift, boost and MFB50 parameters has been conducted in order to maximize the bmep. The engine performance was finally analyzed with the reduced-size turbine. The results of the optimized calibration are reported in Table 9, both for the original turbine configuration and the MFM = 0.8 one.

First of all, as it is usual for high-speed conditions, the target boost pressure is always easily achieved. As expected, a reduced-size turbine leads to a slight decrease in the air-mass flow rate caused by a higher backpressure and finally to a decrease in bmep of around 4%. This seems to be acceptable, in view of the advantages reached at 2000 rpm, thus the

adoption of a smaller turbine represents a good compromise for the engine to be run on hydrogen, with a lean combustion concept.

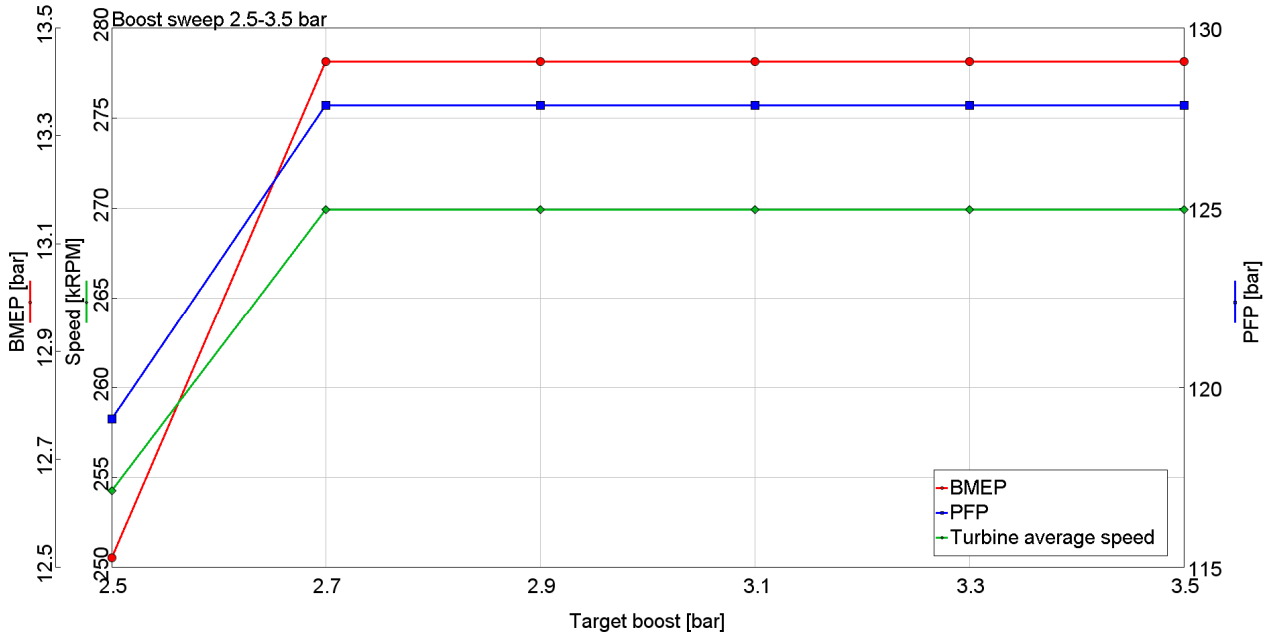

Figure 15. Target boost sweep for the original turbine model at 4000 rpm, full load. MFB50 = 7.1 °CA, nominal IVC = 420 °CA.

Table 9. Results for both the original (MFM = 1.0) and reduced-size turbine (MFM = 0.8) at 4000 rpm, full load. Fixed parameters: MFB50 = 17.9 °CA, nominal IVC = 490 °CA, target boost pressure = 2.3 bar.

MFB50 = 17.9 °CA Nominal Lift = 490 °CA Target Boost = 2.3 bar	Average PFP	bmep	bsec	Boost Pressure	Air Mass Flow Rate	Turbine Inlet Temperature	Turbine Inlet Pressure	Turbine Speed
	bar	bar	MJ/kWh	bar	g/s	K	bar	kRPM
Original turbine	109.0	14.4	10.3	2.30	106.5	939	3.06	265
Turbine MFM = 0.8	107.9	13.8	10.6	2.30	104.6	946	3.42	262
Difference	−1%	−4%	+3%	0%	−2%	+1%	+12%	−1%

6. Conclusions

The present paper presented the results of a feasibility study for a hydrogen-fueled internal combustion engine, aimed at quantifying the fuel impact on the performance, as well as the requirements in terms of engine calibration. The study was carried out in two steps.

The first step was focused on a four-cylinder SI engine featuring an overall displacement of 2000cc. The turbocharger was not included in the model, but the pressure at the model input was imposed so as to reproduce the effect of a compressor. This choice was motivated by the opportunity to maximize the model flexibility and to highlight the ideal requirements for the turbocharger. In the second step, a high-performance prototype 1400cc engine model was calibrated against the available experimental data, under NG fueling, and the performance in the case of hydrogen fueling was analyzed.

Overall, the structure of the present work showed the main limitation that no attention was given to the NOx formation aspect. However, the authors decided to concentrate their attention on a reliable but simple description of the main performance-related variables and their dependence on the fuel characteristics. More in detail, the analysis performed with imposed boost level in the case of Engine #1 allowed a great degree of freedom in the

intake pressure definition, thus setting the limits for an ideal turbocharger group. The work performed on Engine #2 is complementary to the first part from this point of view.

The main results can be summarized as follows.

- In the presence of a fixed PFP limit, the ideal boost level had to be reduced for the H_2 fueling by around 15%. This requirement is particularly strict if the original NG calibration presents extremely large boost level and is one of the reasons behind the detriment in the bmep output.
- In the presence of an ideal supercharging device in both the NG and the H_2 engines, the hydrogen-powered one showed a bmep reduction by around 35% over the entire full-load curve, which is due to both the reduction in the boost level and the decision to run lean. This result was influenced by the absence of turbocharger limitations, which has led to an optimistic bmep curve for the NG engine. However, the absolute value of the H_2 engine bmep, 20 bar, represents a very good result. The better combustion phasing also contributes to an improvement of the specific energy consumption by around 10–15%.
- The results from Engine #2 pointed out a decrease in the achievable bmep by around 7%, which is lower than in Engine #1. The main reasons are (i) a more realistic boost modeling approach, (ii) the high CR of the engine, which limits the maximum achievable boost for both the baseline and the H_2 engine, and (iii) the early IVC adopted at full load combined with late direct injection, which nearly remove the detriments induced by the low hydrogen density.
- A reduction in the turbine size by around 20% was shown to be beneficial in order to maximize the performance at 2000 rpm. The final results from Engine #2 indicate that the lean-burn H_2 engine with smaller turbine can guarantee a bmep output of 16.2 bar, which is in line with the predictions from Engine #1 and indicates promising ground for further optimization of the turbocharger optimization.
- At 4000 rpm, the smaller-size turbine can provide a bmep of 13.8 bar, which is 4% lower than in the case of the original turbine.

Author Contributions: Conceptualization, all authors; methodology, all authors; software, A.S. and M.B., validation, all authors; formal analysis, all authors; investigation, A.S. and M.B., resources, A.S.; data curation, all authors; writing—original draft preparation, A.S. and M.B., writing—review and editing, D.A.M.; supervision, D.A.M. and M.B.; project administration, D.A.M. and M.B. All authors have read and agreed to the published version of the manuscript.

Funding: This research received no external funding.

Data Availability Statement: Data are unavailable due to confidentiality restrictions.

Acknowledgments: The authors acknowledge the valuable contribution of Fiat Research Center, AVL List GmbH and BorgWarner Luxembourg during the Gason research project, whose prototype engine was taken as baseline Engine #2 in this work.

Conflicts of Interest: The authors declare no conflict of interest.

Abbreviations

BEV	Battery Electric Vehicle
BMEP	Brake Mean Effective Pressure
BSEC	Brake Specific Energy Consumption
BSFC	Brake Specific Fuel Consumption
CR	Compression Ratio
DI	Direct Injection
EOI	End Of Injection
FC	Fuel Cell
IVC	Intake Valve Closure
LHV	Lower Heating Value
MBT	Maximum Braking Torque

MFB50	Mass Burned Fraction at 50%
MFM	Mass-Flow Multiplier
NG	Natural Gas
PFP	Peak Firing Pressure
PFI	Port Fuel Injection
RES	Renewable Energy Sources
SI	Spark Ignition
TCO	Total Cost of Ownership
TIT	Turbine Inlet Temperature
TPA	Three Pressure Analysis
VVA	Variable Valve Actuation
Symbols	
λ	Air–fuel equivalence ratio
CH_4	Methane
H_2	Hydrogen

References

1. IPCC. *Climate Change 2023: Synthesis Report*; IPCC: Geneva, Switzerland, 2023.
2. IEA. *World Energy Outlook 2023*; IEA: Paris, France, 2023.
3. IEA. *Energy Technology Perspectives 2023*; IEA: Paris, France, 2023.
4. Verhelst, S.; Wallner, T. Hydrogen-Fueled Internal Combustion Engines. *Prog. Energy Combust. Sci.* **2009**, *35*, 490–527. [CrossRef]
5. Maggio, G.; Nicita, A.; Squadrito, G. How the Hydrogen Production from RES Could Change Energy and Fuel Markets: A Review of Recent Literature. *Int. J. Hydrogen Energy* **2019**, *44*, 11371–11384. [CrossRef]
6. Sens, M.; Danzer, C.; von Essen, C.; Brauer, M.; Wascheck, R.; Seebode, J.; Kratzsch, M. Hydrogen Powertrains in Competition to Fossil Fuel Based Internal Combustion Engines and Battery Electric Powertrains. In Proceedings of the 42nd International Vienna Motor Symposium 2021, Virtual, 29–30 April 2021.
7. Onorati, A.; Payri, R.; Vaglieco, B.M.; Agarwal, A.K.; Bae, C.; Bruneaux, G.; Canakci, M.; Gavaises, M.; Günthner, M.; Hasse, C.; et al. The Role of Hydrogen for Future Internal Combustion Engines. *Int. J. Engine Res.* **2022**, *23*, 529–540. [CrossRef]
8. Exxon Mobil. *The Outlook for Energy: A View to 2040*; ExxonMobil: Spring, TX, USA, 2016.
9. Handwerker, M.; Wellnitz, J.; Marzbani, H. Comparison of Hydrogen Powertrains with the Battery Powered Electric Vehicle and Investigation of Small-Scale Local Hydrogen Production Using Renewable Energy. *Hydrogen* **2021**, *2*, 76–100. [CrossRef]
10. Misul, D.; Baratta, M.; Xu, J.; Fuerhapter, A.; Heindl, R. Experimental and CFD Investigation of Fuel Mixing in an Optical-Access Direct-Injection NG Engine and Correlation with Test Rig Combustion and Performance Data. *Energies* **2023**, *16*, 3004. [CrossRef]
11. Sevik, J.; Pamminger, M.; Wallner, T.; Scarcelli, R.; Reese, R.; Iqbal, A.; Boyer, B.; Wooldridge, S.; Hall, C.; Miers, S. Performance, Efficiency and Emissions Assessment of Natural Gas Direct Injection Compared to Gasoline and Natural Gas Port-Fuel Injection in an Automotive Engine. *SAE Int. J. Engines* **2016**, *9*, 1130–1142. [CrossRef]
12. Verhelst, S. Recent Progress in the Use of Hydrogen as a Fuel for Internal Combustion Engines. *Int. J. Hydrogen Energy* **2014**, *39*, 1071–1085. [CrossRef]
13. Hosseini, S.E.; Butler, B. An Overview of Development and Challenges in Hydrogen Powered Vehicles. *Int. J. Green. Energy* **2020**, *17*, 13–37. [CrossRef]
14. Stępień, Z. A Comprehensive Overview of Hydrogen-Fueled Internal Combustion Engines: Achievements and Future Challenges. *Energies* **2021**, *14*, 6504. [CrossRef]
15. Jilakara, S.; Vaithianathan, J.V.; Natarajan, S.; Ramakrishnan, V.R.; Subash, G.; Abraham, M.; Krishnan Unni, J.; Das, L.M. An Experimental Study of Turbocharged Hydrogen Fuelled Internal Combustion Engine. *SAE Int. J. Engines* **2015**, *8*, 314–325. [CrossRef]
16. Sopena, C.; Diéguez, P.M.; Sáinz, D.; Urroz, J.C.; Guelbenzu, E.; Gandía, L.M. Conversion of a Commercial Spark Ignition Engine to Run on Hydrogen: Performance Comparison Using Hydrogen and Gasoline. *Int. J. Hydrogen Energy* **2010**, *35*, 1420–1429. [CrossRef]
17. Bao, L.-Z.; Sun, B.-G.; Luo, Q.-H.; Li, J.-C.; Qian, D.-C.; Ma, H.-Y.; Guo, Y.-J. Development of a Turbocharged Direct-Injection Hydrogen Engine to Achieve Clean, Efficient, and High-Power Performance. *Fuel* **2022**, *324*, 124713. [CrossRef]
18. Zhao, H. *Advanced Direct Injection Combustion Engine Technologies and Development*; Woodhead Publishing: Sawston, UK, 2010; Volume 1.
19. Douailler, B.; Ravet, F.; Delpech, V.; Soleri, D.; Reveille, B.; Kumar, R. Direct Injection of CNG on High Compression Ratio Spark Ignition Engine: Numerical and Experimental Investigation. In Proceedings of the SAE 2011 World Congress & Exhibition, Detroit, MI, USA, 12–14 April 2011.
20. Adlercreutz, L.; Cronhjort, A.; Andersen, J.; Ogink, R. Optimizing the Natural Gas Engine for CO_2 Reduction. In Proceedings of the SAE 2016 World Congress and Exhibition, Detroit, MI, USA, 12–14 April 2016.
21. Baratta, M.; Misul, D. Development of a Method for the Estimation of the Behavior of a CNG Engine over the NEDC Cycle and Its Application to Quantify for the Effect of Hydrogen Addition to Methane Operations. *Fuel* **2015**, *140*, 237–249. [CrossRef]

22. Kim, J.; Chun, K.M.; Song, S.; Baek, H.K.; Lee, S.W. The Effects of Hydrogen on the Combustion, Performance and Emissions of a Turbo Gasoline Direct-Injection Engine with Exhaust Gas Recirculation. *Int. J. Hydrogen Energy* **2017**, *42*, 25074–25087. [CrossRef]
23. Baratta, M.; Chiriches, S.; Goel, P.; Misul, D. CFD Modelling of Natural Gas Combustion in IC Engines under Different EGR Dilution and H2-Doping Conditions. *Transp. Eng.* **2020**, *2*, 100018. [CrossRef]
24. Kalam, M.A.; Masjuki, H.H. An Experimental Investigation of High Performance Natural Gas Engine with Direct Injection. *Energy* **2011**, *36*, 3563–3571. [CrossRef]
25. Baratta, M.; Misul, D.; Xu, J.; Fuerhapter, A.; Heindl, R.; Peletto, C.; Preuhs, J.; Salemi, P. Development of a High Performance Natural Gas Engine with Direct Gas Injection and Variable Valve Actuation. *SAE Int. J. Engines* **2017**, *10*, 2535–2551. [CrossRef]
26. Krishnan Unni, J.; Bhatia, D.; Dutta, V.; Das, L.M.; Jilakara, S.; Subash, G. Development of Hydrogen Fuelled Low NOx Engine with Exhaust Gas Recirculation and Exhaust after Treatment. *SAE Int. J. Engines* **2017**, *10*, 46–54. [CrossRef]
27. Mohammadi, A.; Shioji, M.; Nakai, Y.; Ishikura, W.; Tabo, E. Performance and Combustion Characteristics of a Direct Injection SI Hydrogen Engine. *Int. J. Hydrogen Energy* **2007**, *32*, 296–304. [CrossRef]
28. Verhelst, S.; Maesschalck, P.; Rombaut, N.; Sierens, R. Increasing the Power Output of Hydrogen Internal Combustion Engines by Means of Supercharging and Exhaust Gas Recirculation. *Int. J. Hydrogen Energy* **2009**, *34*, 4406–4412. [CrossRef]
29. Rezaei, R.; Kovacs, D.; Hayduk, C.; Mennig, M.; Delebinski, T. Euro VII and Beyond with Hydrogen Combustion for Commercial Vehicle Applications: From Concept to Series Development. *SAE Int. J. Adv. Curr. Pract. Mobil.* **2021**, *4*, 559–569. [CrossRef]
30. Bulgarini, M.; Della Torre, A.; Barillari, L.; Montenegro, G.; Onorati, A.; Gullino, F.; Tonelli, R. Towards H2 High-Performance IC Engines: Strategies for Control and Abatement of Pollutant Emissions. In Proceedings of the 16th International Conference on Engines & Vehicles, Naples, Italy, 28 August 2023.
31. Wallner, T.; Matthias, N.S.; Scarcelli, R.; Kwon, J.C. Evaluation of the Efficiency and the Drive Cycle Emissions for a Hydrogen Direct-Injection Engine. *Proc. Inst. Mech. Eng. Part D: J. Automob. Eng.* **2013**, *227*, 99–109. [CrossRef]
32. Gamma Technologies. *GT-Suite Engine Performance Application Manual*; Gamma Technologies: Westmont, IL, USA, 2022.
33. Gamma Technologies. *GT-Suite Flow Theory Manual*; Gamma Technologies: Westmont, IL, USA, 2022.
34. Heywood, J.B. *Internal Combustion Engine Fundamentals*, 2nd ed.; McGraw-Hill: New York, NY, USA, 2019.